



## **Resolving distortion between linear and area sensors for forensic print inspection**

Stephen B. Pollard, Guy B. Adams, Steven J. Simske

HP Laboratories  
HPL-2010-172

### **Keyword(s):**

Security printing, forensic imaging, anti-counterfeiting, inspection

### **Abstract:**

Forensic analysis of individual printed items, including single characters, provides a readily-integrated means to extend security to any printed item (label, document, package, etc.). In this paper we demonstrate, for the first time, forensic levels of image inspection for workflows involving two very different high-resolution imaging devices, the Dyson Relay CMOS Imaging Device (DrCID) and a high speed line-scan camera. In particular, we show how a similarity metric can be used to identify specific characters with less than 1 in  $10^9$  chance of false matching, while closing the loop between in-line (production) using the line-scan camera and end-user (investigative) inspection with DrCID.

External Posting Date: October 21, 2010 [Fulltext]      Approved for External Publication  
Internal Posting Date: October 21, 2010 [Fulltext]  
Presented at IEEE ICIP 2010 Hong Kong, September, 27, 2010

© Copyright IEEE ICIP 2010,

# RESOLVING DISTORTION BETWEEN LINEAR AND AREA SENSORS FOR FORENSIC PRINT INSPECTION

Stephen B. Pollard<sup>1</sup>, Guy B. Adams<sup>1</sup>, Steven J. Simske<sup>2</sup>

<sup>1</sup>Hewlett Packard Laboratories, Long Down Avenue, Stoke Gifford, Bristol, BS34 8QZ, UK

<sup>2</sup>Hewlett Packard Laboratories, 3404 E. Harmony Rd., MS 36, Fort Collins CO 80528, USA

## ABSTRACT

Forensic analysis of individual printed items, including single characters, provides a readily-integrated means to extend security to any printed item (label, document, package, etc.). In this paper we demonstrate, for the first time, forensic levels of image inspection for workflows involving two very different high-resolution imaging devices, the Dyson Relay CMOS Imaging Device (DrCID) and a high speed line-scan camera. In particular, we show how a similarity metric can be used to identify specific characters with less than 1 in  $10^9$  chance of false matching, while closing the loop between in-line (production) using the line-scan camera and end-user (investigative) inspection with DrCID.

*Index Terms*— Forensic imaging, security, authentication, counterfeit detection, dynamic time warping.

## 1. INTRODUCTION

Counterfeiting, warranty fraud, product tampering, smuggling, product diversion and other forms of organized deception are driving the need for improved brand protection. The potential for security printing and imaging to provide forensic levels of authentication has long been recognized and offers potential to form part of the approach to product and document security [1].

We have previously [2] demonstrated the utility of a low-cost USB-powered mini-appliance (Figure 1a) capable of resolving spatial features of 3.8 microns with 1:1 magnification. This is accomplished using a single Dyson relay lens in series with a mirror and a low cost 3-5 Mpixel CMOS image sensor. With a self-contained (white LED) illumination source, this Dyson relay CMOS imaging device (DrCID) affords the capture of individual typed characters with printing “parasitics”—such as the absorbance of ink into the fibers of the substrate (e.g. paper, cardstock, etc.) along with the droplet “tails” that exhibit micro-random aberrations as shown in Figure 2.

The forensic inspection process requires that a registry of image data (raw or processed to extract a simpler feature based description) is stored in a central repository. The DrCID device, out in the field, can then access the

centralized (generally web based) registry to make a forensic comparison (perhaps making use of a cloud service for the actual processing). In order to achieve a robust and practical solution, it is beneficial if the registry can be built real-time during print production. Here we demonstrate a prototype end-to-end solution where printed media is scanned at speed as part of an ‘inline’ print process.

This is achieved with a high speed line-scan camera mounted above the output tray of an adapted HP K5400 office printer (Figure 1b). Currently we use an E2V 12K element 5um pixel linear monochrome sensor that operates at 27K lines/s (0.14m/s max theoretical surface speed) with 1:1 optics. The experimental rig also features a high intensity halogen light source to enable exposure times shorter than the line period in order to minimize motion blur as the paper passes beneath it during the full speed page feed. While the motion of the paper as it passes beneath the camera is reasonably constant, variations in gear timing, paper slip and vibrations can cause periodic small-scale perturbation in both the lateral and vertical motions of the paper. These variations are significant enough to produce problems for existing approaches to forensic image analysis. Here we present a number of experiments that show how these deficiencies can be overcome in practice.

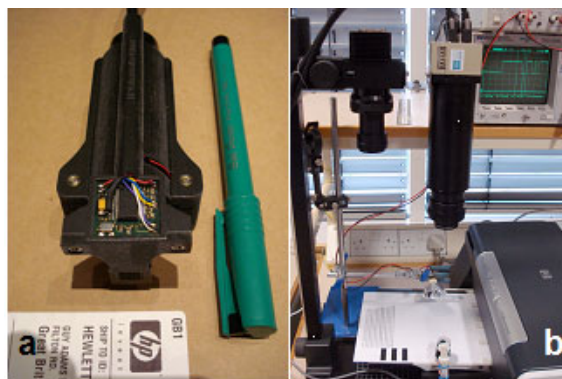


**Figure 1.** (a) shows DrCID with imaging window on the bottom edge; (b) is our experimental inline print and line-scan solution.

Previous work in this area has been limited to pairs of images captured by a single class of imaging device. An early example [3] recovers a print signature from low-cost digital optical-microscopes based on the radius profiles of

binarized circular blobs (of physical diameter 0.07mm) averaged over up to 72 sectors of the circle (measured w.r.t. the centre of gravity of the blob). The blobs were located and registered using fiducial marks and compared based on a Euclidian distance metric. Previous work [2] with DrCID explored the use of any individual printable glyph or character as a forensic mark. Similar to [3] forensic authentication was based on the analysis of the perimeter of thresholded binary image components (in this case over 360 1° bins), but with a number of extra profile measures in addition to radius. Each pair of profiles was aligned to optimize the following normalized similarity metric:

$$S = 1 - (\text{SAD}) / ((\text{SA1} + \text{SA2}) / 2)$$

Where SAD is the sum of absolute differences and SA1 and SA2 are the sum of absolute values of the first and second profile measure respectively.

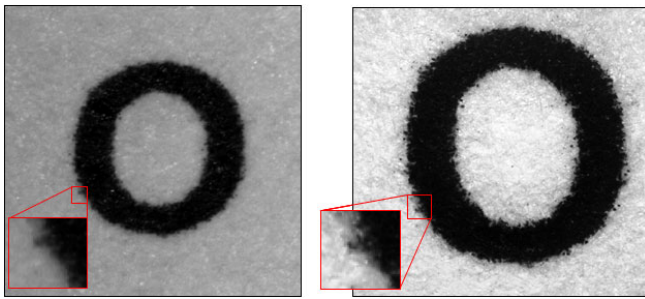


**Figure 2.** An Arial 12 point ‘o’ captured by prototype inline device is shown on the left and by DrCID on the right. Note that the latter is taller, higher resolution and better focused. A perimeter detail is highlighted to show how it is preserved between the two devices.

## 2. METHOD

Figure 2 shows a 12 point ‘o’ character imaged by the inline and DrCID devices. Figure 3 shows the performance difference between inter-device (inline to DrCID) and intra-device (pairs from a single DrCID) forensic comparisons

using a profile signature and matching method that is consistent with the prior art. Each case is based on the same batch of 5 characters simultaneously captured (printed and scanned) by the inline device. Performance of the inter-device end-to-end solution is much degraded with respect to what can be achieved using only the high-quality images from DrCID. Significant systematic errors dominate because of important deficiencies of the inline solution that are discussed in the table below along with proposed solutions.

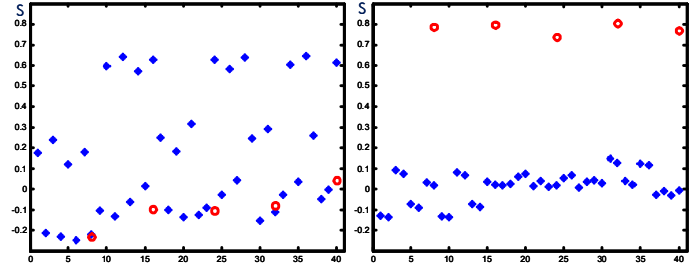


**Figure 3.** Each graph plots the similarity S for a number of experimental trials based on 2 scans of 5 individual characters. Veridical matches (red circles) and false associations (blue stars) for inter-device comparisons on the left and intra-device (DrCID only) comparisons on the right.

### 2.1. Forensic comparison

Our approach to the extraction and matching of signature profiles from the two devices is outlined in the algorithm described on the next page. Figure 4 (top) shows an ellipse model fitted to another pair of 12 point ‘o’ characters. Note that the model is not a perfect fit to shape of the character but it does allow for the first order linear deformation of the shape due to poor control of the average speed of the printer and the alignment of the line-scan sensor. Figure 4 also shows how the residual systematic errors in the extracted signature profiles between the two imaging devices can be resolved by high-pass filtering the recovered signal and using a form of variable penalty Dynamic Time Warping (DTW) [5] to deal with the temporal miss-alignment.

Problem	Discussion	Solution
<b>Linear distortion</b>	An affine distortion of the inline image results from calibration and alignment error of the line-scan camera and variability in the sustained speed of the paper flow. This must be modeled in order to bring the two print signatures into better correspondence.	By restricting our attention to ‘o’ type glyphs that can be closely modeled as circles or ellipses, we reduce the problem to one of ellipse fitting (using linear least squares [4]) as the affine transform of an ellipse is also an ellipse. While not a general solution, this is a sufficient basis for the experiments presented here.
<b>Scale and focus difference</b>	Even though all measures are normalized to the scale of the extracted glyph, it helps to process the higher resolution, better focused version to better match the spatial frequency content of the inferior device.	In these experiments, we apply a 2D Gaussian smoothing filter to the high resolution image to approximate the change in resolution and poorer focus of the low resolution version. More sophisticated solutions are clearly possible.
<b>Residual non-linear error</b>	Finally we must deal with residual non-linear errors resulting from limitations of the linear correction. This can be broken into two components: one lateral to the measured border that causes a low frequency amplitude error and one along the perimeter that distorts the index/timeline of the signature profile.	The lateral amplitude error can be resolved by high pass filtering the signature profile by subtracting a 1D Gaussian smoothed version. Correction of the distorted time index is achieved using a novel form of variable penalty Dynamic Time Warping (DTW) that also includes a penalty term dependent on the degree of warping.

### Algorithm for Forensic Comparison

1. Compute signature profiles for inline & DrCID imagers:
  - a. Use adaptive thresholding to identify the text glyph.
  - b. Fit ellipse model to the outer edge.
  - c. Extract size-normalized 1D intensity profile in the direction normal to the ellipse contour.
  - d. Compute location measure over the extracted profile (binary image edge in the simplest case).
  - e. Use high pass filter to remove the residual errors.
2. Match the signature profiles:
  - a. Consider all possible rotations.
  - b. Minimize the sum of absolute difference (SAD).
  - c. Use DTW to improve SAD metric.
  - d. Compute similarity metric  $S$  based on SAD.
3. If  $S > T$  (Similarity Threshold) then forensic match established.

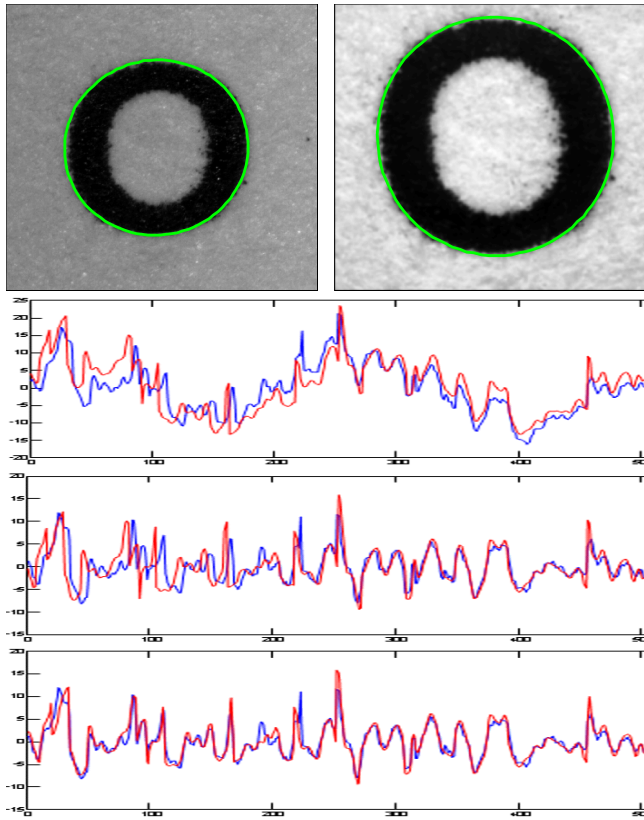


**Figure 4.** Top again shows an Arial 12 point ‘o’ captured by prototype inline device on the left and DrCID on the right. In this case the latter is Gaussian smoothed (sigma = 3.0) to match better the frequency content of the former. Each is fitted with an ellipse model. Three successive graphs show a subset of a 1000 element signature profile measured normal to the ellipse contour. The first shows a significant systematic error due to deficiencies in the model and residual non-linear distortion which can be resolved by first high-pass filtering (middle graph) and finally Dynamic Time Warping (bottom graph). Note that the residual misalignment of the signals is nicely resolved by these techniques.

### 2.2. Dynamic Time Warping

The novel form of variable penalty DTW necessary to achieve the required authentication accuracy and is outlined figure 5. It is novel in that it exploits the slow and smooth warping of time with respect to the signature profile. Rather than allowing time to be warped discontinuously at the scale of the signal measurement (as is usually the case with DTW) two sampling frequencies are chosen: a coarse one to define the steps over which time can reasonably be modeled as a linear function; and a much finer one based on the sampling rate of the signal. Furthermore a much more meaningful variable warp penalty (related directly to the degree of linear distortion) can be introduced at each step to give preference to the more likely deformations.

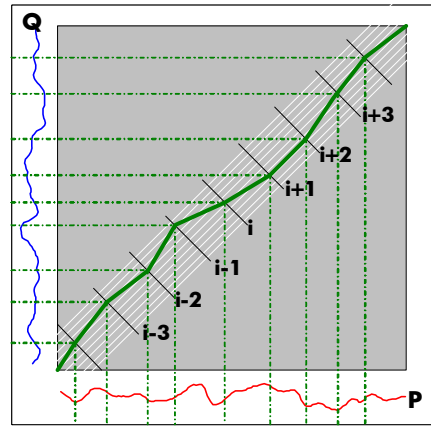


**Figure 5.** Outlines the novel DTW scheme. Two signals, P and Q are to be matched. The stages  $i$  represent a coarse quantization of time. At each stage the path (example shown thick green in the image) must pass through a white diagonal ‘sampling’ control point. At each step there are a limited number of options that define linear interpolations of respective intervals of P and Q. A step along a diagonal implies a direct mapping with no distortion. A step up to the next higher diagonal gives rise to a one unit expansion of the time interval in Q and a corresponding one unit compression in P. Conversely a step to the next lower diagonal has the opposite effect. At each stage a distortion limit ( $\pm n$ ) is imposed on the size of off diagonal step. Using also the standard Sakoe-Chiba limit on the maximum allowed deviation [6] the cost of all allowable steps is computed once and then dynamic programming is used to determine the optimal path.

The recurrence update of the dynamic programming is thus:

$$C_{i,j} = \min_{k \in [-n..n]} (C_{i-1,j+k} + c(i,j,k) + \lambda k)$$

where  $i$  is the temporal stage,  $j$  is the current diagonal,  $k$  is the relative diagonal step over the allowed range  $n$  with respect to the previous time step ( $i-1$ ),  $c(i,j,k)$  is the cost of matching P and Q (in this case the  $L_1$  norm after linear interpolation to a common constant sample count) over the intervals defined by  $i$ ,  $j$  and  $k$  and  $\lambda$  is a regularizing parameter for the degree of deformation  $k$  that provides the variable warp penalty. In our experiments at most 33 time stages were chosen to cover the signature profile and the relative diagonal step  $n$  is limited to one third the time step.

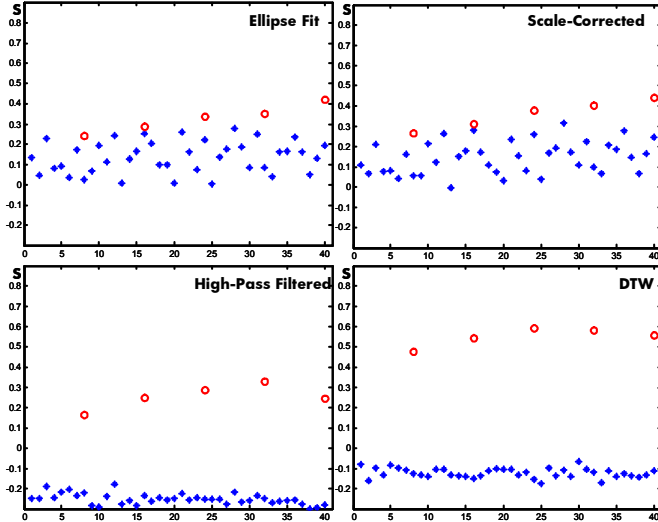


**Figure 6.** The same inter-device comparison reported in figure 3 is improved top left to bottom right. At each step a new element of the solution is added. While scale correction makes only a modest improvement in isolation it is essential for the subsequent gains.

#### 4. RESULTS

Figure 6 illustrates how the authentication accuracy improves as each aspect of the solution is added. Population statistics recovered from pooled data over numerous trials (i.e. capturing inline and corresponding DrCID images of ‘o’ characters) are presented in figure 7 for a wide range of parameter settings. In each case we plot a simple statistical separation metric  $Z$

$$Z = \frac{|\bar{S}_V - \bar{S}_F|}{\sigma_V + \sigma_F}$$

that is the absolute difference of the similarity metric means over the sum of their standard deviations for respective distributions of veridical and false matches. This is called  $Z$  as it corresponds to a point of equal Z-Score between two Gaussian distributions. The peak statistical separation in our experiments is over 11.1 which corresponds to an infinitesimally small probability if the distributions truly are Gaussian (above 6 corresponds to a probability of  $1 \times 10^{-9}$ ) and indicates a robust statistical difference even if they are not. We have also experimented with more sophisticated grayscale location measures that are more robust to illumination variation than binary thresholding but as the combined DTW based metric is also robust to these variations we obtain no overall improvement in practice for this data.

#### 4. DISCUSSION

We have shown that it in order to perform closed loop forensic verification of printed inkjet characters, it is necessary to overcome 4 important limitations of the imaging process of the inline solution: linear distortion,

spatial frequency difference, non-linear amplitude error and temporal mismatch. In order achieve forensic authentication accuracy, a novel and useful form of DTW has been developed and presented here for the first time. Importantly, and unlike previous solutions, we have adopted a model-based approach that separates the truly random part of the outline of the individual printed character from the shared shape-conveying component. Furthermore, forensic level authentication has been achieved between the very different optical devices with the minimum of engineering effort and cost: we neither need to use accurate calibration nor precise monitoring of the paper motion past the line-scan device.

Clearly, the problem has been simplified by using a symmetric character as the basis of the experimentation. Also there is an issue in that it was necessary to compensate for the difference in spatial frequency content between the two devices. While for some applications these issues may not be a problem we plan to extend our work to deal with a wide variety of printed characters or otherwise shape-model amenable glyphs and explore other device combinations.

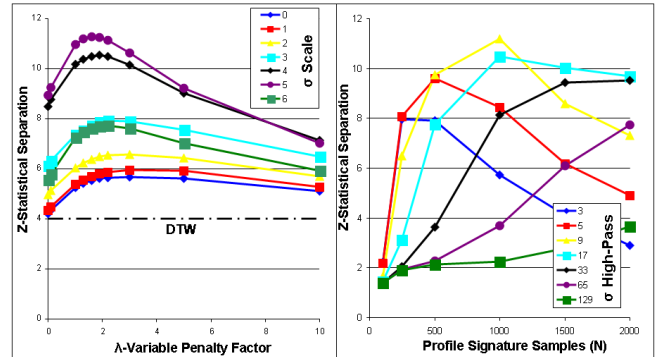


**Figure 7.** Graph (left) plots  $Z$  against variable penalty factor  $\lambda$  for a range of Gaussian smoothing of the DrCID image ( $\sigma$  Scale). Graph (right) plots  $Z$  against the number of profile samples  $N$  for choices of high-pass filter of the signature profile ( $\sigma$  High-Pass). In combination this would suggest a good set of parameters ( $\lambda = 1.3$ ,  $\sigma_S = 5$ ,  $N = 1000$ ,  $\sigma_{HP} = 9$ ). The best performance for a standard DTW is also shown for comparison.

#### 5. REFERENCES

- [1] D. Pizzanelli, *The Future of Anti-Counterfeiting, Brand Protection and Security Packaging V*, Pira International Ltd., Leatherhead, UK, 2009. (see <http://www.intertechpira.com>)
- [2] S.J. Simske and G. Adams, “High-Resolution Glyph-Inspection Based Security System”, *IEEE ICASSP*, pp. 1794-1797, 2010.
- [3] B. Zhu, J. Wu and M.S. Kankanhalli, “Print Signature for Document Authentication”, *ACM CCS*, pp 145-154, 2003.
- [4] A.W. Fitzgibbon, M. Pilu, and R. B. Fischer, “Direct least squares fitting of ellipses”. *ICPR13*, pp 253-257, 1996.
- [5] D. Clifford, G. Stone, I. Montoliu, S. Rezzi, F.P. Martin, P. Guy, S. Bruce and S. Kochhar, “Alignment Using Variable Penalty Dynamic Time Warping”, *Anal. Chem.* 81, pp 1000-1007, 2009.
- [6] H. Sakoe and S. Chiba, “Dynamic Programming Optimization for Spoken Word Recognition”, *IEEE Trans. Acoust., Speech, Signal Process.*, 26(1), pp 43-49, 1978.